Journal of Power Sources 196 (2011) 1433–1441

Contents lists available at ScienceDirect

Journal of Power Sources

journal homepage: www.elsevier.com/locate/jpowsour

One ether-functionalized guanidinium ionic liquid as new electrolyte for lithium battery

Shaohua Fang [a], Yufeng Tang [a], Xingyao Tai [a], Li Yang [a,*], Kazuhiro Tachibana [b], Kouichi Kamijima [c]

[a] School of Chemistry and Chemical Technology, Shanghai Jiaotong University, No. 800, Dongchuan Road, MinHang District, Shanghai 200240, China
[b] Department of Chemistry and Chemical Engineering, Faculty of Engineering, Yamagata University, Yamagata 992-8510, Japan
[c] Hitachi Chemical Co. Ltd., Ibaraki-ken 317-8555, Japan

ARTICLE INFO

Article history:
Received 1 December 2009
Received in revised form 9 August 2010
Accepted 11 August 2010
Available online 17 August 2010

Keywords:
Lithium battery
Ionic liquid
Electrolyte
Ether-functionalized guanidinium cation

ABSTRACT

One ether-functionalized guanidinium ionic liquid is used as new electrolytes for lithium battery. Viscosity, conductivity, behavior of lithium redox, chemical stability against lithium metal, and charge–discharge characteristics of lithium batteries, are investigated for the IL electrolytes with different concentrations of lithium salt. Though the cathodic limiting potential of the IL are 0.7 V vs. Li/Li^+, the lithium plating and striping on Ni electrode can be observed in the IL electrolytes, and the IL electrolytes show good chemical stability against lithium metal. $Li/LiCoO_2$ cells using the IL electrolytes without additives have good capacity and cycle property at the current rate of 0.2 C when the LiTFSI concentration is higher than 0.3 mol kg^{-1}, and the cell using the IL electrolyte with 0.75 mol kg^{-1} LiTFSI owns good rate property. The activation energies of the $LiCoO_2$ electrode for lithium intercalation are estimated, and help to analyze the factors determining the rate property.

1. Introduction

Ionic liquids (ILs) are molten salts with melting points at or below ambient temperature, and they have some unique properties, including good electrochemical and thermal stability, high ionic conductivity, non-volatility and nonflammability [1,2]. Due to these properties, ILs have showed potential as safe electrolytes for being applied in high-energy-density lithium battery system, which uses lithium metal anode with high theoretical capacity (more than 3860 mAh g^{-1}) [3–6]. Furthermore, IL or IL-polymer electrolytes can obviously improve the performance of lithium battery using some cathode materials with high theoretical capacity (such as S [7,8], NiS–Ni_7S_6 [9], V_2O_5 [10] and LiV_3O_8 [11]), owing to reduced dissolution of the active material into electrolytes compared with organic electrolytes.

The ILs, which have been used as electrolytes for lithium battery, can be classified into two categories according to their electrochemical stability. The first category contains tetraalkylammonium, pyrrolidinium, piperidinium and quaternary phosphonium ILs, which have better electrochemical stability and possess sufficiently lower cathodic limiting potentials to allow the deposition of lithium [12–14]. For example, N-methyl-N-propylpiperidinium bis(trifluoromethanesulfonyl)imide (PP13-TFSI) N-methyl-N-propylpyrrolidinium bis(fluorosulfonyl)imide (P13-FSI), N,N-diethyl-N-methyl-N-(2-methoxyethyl) ammonium bis(trifluoromethanesulfonyl)imide (DEME-TFSI) and triethyl(2-methoxyethyl) phosphonium bis(trifluoromethanesulfonyl)imide (P222(2o1)-TFSI) have been reported to own good cycle performance when they are used in lithium battery at low rate without additives [3,4,15–20]. The second category includes imidazolium and guanidinium ILs, which have narrower electrochemical windows and higher cathodic limiting potentials compared with the first category. However, some ILs in the second category still have chances to be used in lithium battery successfully, because of the forming of good SEI (solid electrolyte interphase) film on lithium metal, which can restrain the reduction of IL electrolytes and allow the deposition of lithium. The electrolyte without additives based on 1-ethyl-3-methyl imidazolium bis(fluorosulfonyl)imide (EMI-FSI) has been used in lithium battery [4]. The introduction of alkyl groups on the C-2 position of the imidazolium ring can improve the electrochemical stability of ILs [21,22], and 1,2-dimethyl-3-propyl imidazolium bis(trifluoromethanesulfonyl)imide (DMPIm-TFSI) electrolyte can be used in lithium battery without additives [23]. A series of guanidinium ILs based on small cations and TFSI anion have been synthesized by our group, and it has been found that two guanidinium ILs (1g13-TFSI and 1g22-TFSI), which have similar cathodic limiting potentials to the ILs based on EMI cation, can also be used as electrolytes for lithium battery without additives [24,25].

* Corresponding author. Tel.: +86 21 54748917; fax: +86 21 54741297.
E-mail address: liyangce@sjtu.edu.cn (L. Yang).

0378-7753/$ – see front matter © 2010 Elsevier B.V. All rights reserved.
doi:10.1016/j.jpowsour.2010.08.012

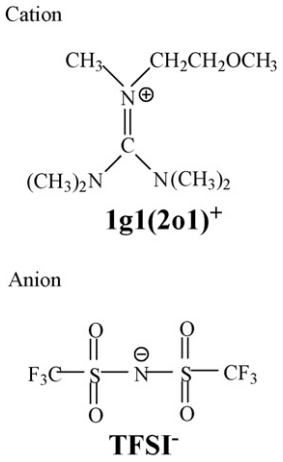

Fig. 1. Structures of cation and anion of this functionalized guanidinium IL used in this study.

Recently, eight functionalized guanidinium ILs based on small cations with ether group (methoxyethyl group, $CH_3OCH_2CH_2$) or ester group (methyl acetate group) and TFSI anion have been prepared by our group [26]. In this study, one ether-functionalized guanidinium IL with low viscosity was used as new electrolyte for $Li/LiCoO_2$ cell without additives, and the relationship between the electrolyte characteristics and the performances of $Li/LiCoO_2$ cells were studied more detailedly. Viscosity, conductivity, behavior of lithium redox on Ni electrode and chemical stability against lithium metal, were investigated for the IL electrolytes with different concentrations of lithium salt. We examined the charge–discharge characteristics for the $Li/LiCoO_2$ cells using the IL electrolytes, and estimated the activation energies of the $LiCoO_2$ electrode for lithium intercalation by electrochemical impedance spectra (EIS) method. And we found that, the cells had good capacity and cycle property at the current rate of 0.2 C when the LiTFSI concentration in the IL electrolyte was higher than 0.3 mol kg^{-1}, and the cell using the IL electrolyte with 0.75 mol kg^{-1} LiTFSI owned good rate property.

2. Experimental

The structure of this functionalized guanidinium IL used in this study was shown in Fig. 1, and the IL was prepared according to our reported method [26]. The IL was dried under high vacuum for more than 24 h at 100 °C before using. The water content of the dried IL was detected by a moisture titrator (Metrohm 73KF coulometer) based on Karl–Fischer method, and the value was less than 50 ppm. Then five concentrations (0.3, 0.45, 0.6, 0.75 and 0.9 mol kg^{-1}) of LiTFSI (kindly provided by Morita Chemical Industries Co., Ltd.), were added to the dried IL, respectively. And this procedure was carried out in an argon-filled glove box ($[O_2] < 1$ ppm, $[H_2O] < 1$ ppm).

The viscosities of the IL electrolytes were measured with viscometer (DV-III ULTRA, Brookfield Engineering Laboratories, Inc.), and the conductivities were got by using DDS-11A conductivity meter.

Electrochemical window of the IL was measured by linear sweep voltammogram (LSV) in the glove box. The working electrode was glassy carbon disk (3 mm diameter), and lithium metal was used as both counter and reference electrodes. The plating and stripping behaviors of lithium in the IL electrolytes were examined by using cyclic voltammogram (CV) method in the glove box. The nickel disk (2 mm diameter) was used as the working electrode, and lithium metal was used as both counter and reference electrodes.

Table 1
Viscosity and conductivity of 1g1(2o1)-TFSI and its IL electrolytes with different concentrations of LiTFSI at 25 °C.

	Viscosity (mPa s)	Conductivity (mS cm^{-1})
1g1(2o1)-TFSI	58	2.15
0.3 mol kg^{-1} LiTFSI in 1g1(2o1)-TFSI	110	1.19
0.45 mol kg^{-1} LiTFSI in 1g1(2o1)-TFSI	147	0.89
0.6 mol kg^{-1} LiTFSI in 1g1(2o1)-TFSI	195	0.67
0.75 mol kg^{-1} LiTFSI in 1g1(2o1)-TFSI	268	0.49
0.9 mol kg^{-1} LiTFSI in 1g1(2o1)-TFSI	316	0.36

The Ni electrode was polished with alumina paste ($d = 0.1$ μm). And the polished electrode was washed with deionized water and dried under vacuum. The linear sweep voltammogram and cyclic voltammogram were performed by CHI 604b electrochemistry workstation at room temperature (25 °C).

The stability of the IL electrolyte against lithium at room temperature was investigated by monitoring the time evolution of the impedance response for a symmetric Li/IL electrolyte/Li coin cell with the borosilicate glass separator (GF/A from Whattman), and the impedance responses were measured by using CHI 604b electrochemistry workstation (100 kHz to 50 mHz; applied voltage 5 mV).

$Li/LiCoO_2$ coin cell was used to evaluate the performances of the IL electrolytes in lithium battery applications. Lithium metal was used as anode. And cathode was fabricated by spreading the mixture of $LiCoO_2$, acetylene black and PVDF (initially dissolved in N-methyl-2-pyrrolidone) with a weight ratio of 8:1:1 onto Al current collector (battery use). Loading of active material was about ca. 1.0–1.5 mg cm^{-2} and this thinner electrode was directly used without pressing. The separator was also glass filter made of borosilicate glass (GF/A from Whattman). Cell construction was carried out in the glove box, and all the components of cell were dried under vacuum before placed into the glove box. The cells were sealed and then stayed at room temperature for 4 h before performance test. The cell performances were examined by the galvanostatic charge–discharge (C–D) cycling test using a CT2001A cell test instrument (LAND Electronic Co., Ltd.) at room temperature. Current rate was determined by using the nominal capacity of 150 mAh g^{-1} for $Li/LiCoO_2$ cell. Charge included two processes: (1) constant current at a rate, cut-off voltage of 4.2 V, (2) constant voltage at 4.2 V, cut-off current of 0.01 mA, and discharge had one process: constant current at the same rate, cut-off voltage of 3.2 V.

The impedance responses of $Li/LiCoO_2$ coin cells with the IL electrolytes, were measured by using CHI 604b electrochemistry workstation (100 kHz to 50 mHz; applied voltage 5 mV). Prior to the impedance measurement, the coin cells were discharged to 3.85 V vs. Li/Li^+ after four charge–discharge cycles at 0.2 C current rate, and held for 10 min to reach the equilibrium state at 20, 25 and 30 °C.

3. Results and discussion

3.1. Viscosities and conductivities of the IL electrolytes

The viscosities and conductivities of 1g1(2o1)-TFSI and its IL electrolytes with different concentrations of LiTFSI at room temperature are listed in Table 1. The viscosity of the ether-functionalized guanidinium IL in this study was 58 mPa s at 25 °C. Compared with the other ILs which have been used in lithium battery without additives, the viscosity of the IL was slightly higher than EMI-FSI, P13-FSI and P222(2o1)-TFSI, and lower than PP13-TFSI, DEME-

TFSI and several other quaternary ammonium-based ILs [3,4,14,20]. The viscosity increased and conductivity decreased after dissolving Lithium salts in this IL. When the LiTFSI concentration increased from 0.3 to 0.9 mol kg^{-1}, the viscosity of IL electrolyte increased and the conductivity decreased markedly. For the IL electrolyte with 0.9 mol kg^{-1} LiTFSI at 25 °C, the viscosity was 316 mPa s, and the conductivity was only 0.36 mS cm^{-1}.

For BMI-TFSI, BDMI-TFSI, BMP-TFSI and DEME-TFSI, the conductivity of IL electrolyte also decreased with the increasing of LiTFSI concentration [27–29]. The diffusion coefficients of ions in these IL electrolytes were measured by the method of pulsed field gradient NMR, and some experimental results were discovered that: (1) the diffusion coefficients of organic cation and anion in IL decreased after the addition of lithium salt with same anion as IL; (2) the diffusion coefficient of the lithium ion was obviously lower than organic cation and anion; (3) the diffusion coefficients of all ionic species decreased with the increasing of lithium salt concentration [27–29]. Based on the above results, the decreasing of conductivity with the increasing of LiTFSI concentration in 1g1(2o1)-TFSI electrolytes could be explained as follows: the lithium ion owning small size and high positive density had stronger coulomb interaction with the anion than the organic cation, which resulted in the low mobility of the lithium ion and the decreased mobility of the anion after the addition of lithium salt with same anion as IL; the coulomb interaction between the organic cation and the anion also turned stronger due to the increasing of the anion concentration after the addition of lithium salt with same anion as IL, which resulted in the decreasing mobility of the organic cation; the decreasing mobility of all the ionic species should cause the decreasing of conductivity with the increasing of lithium salt concentration. Although the increasing of viscosity could not be directly explained by the decreasing mobility of the ionic species, the addition of lithium salt and the stronger interaction between the cations and the anions might change the configurations of ion pairs or complexes in IL electrolyte, which was possible to cause viscosity to increase. Certainly, the low mobility of the lithium ion in electrolyte should have negative effect on the rate property of lithium battery, due to the restriction of lithium ion transport at high current rate.

The temperature dependence of viscosity was investigated for 1g1(2o1)-TFSI and its IL electrolytes with different concentrations of LiTFSI over the temperature range 25–80 °C, and the VTF plots of viscosity according to Eq. (1) were shown as examples in Fig. 2.

$$\eta = \eta_0 \exp\left(\frac{B}{T - T_0}\right) \quad (1)$$

η_0 (mPa s), B (K) and T_0 (K) are constants of this equation, and these three values and the VTF fitting parameter (R^2) for the IL and its IL electrolytes were calculated and listed in Table 2. According to Fig. 2 and the values of R^2 in Table 2, they were very well fit by the VTF model over the temperature range studied.

According to Table 2, it was found that the η_0 value of 1g1(2o1)-TFSI was bigger than its IL electrolytes with different concentrations of LiTFSI. And the IL had the smaller B and T_0 value compared with its IL electrolytes. However, the η_0, B and T_0 values of the IL electrolytes did not have explicit relationship with the concentrations of LiTFSI.

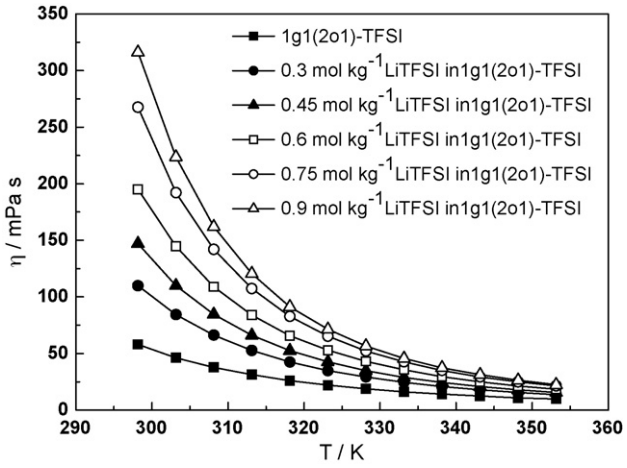

Fig. 2. Change of viscosity with temperature for 1g1(2o1)-TFSI and its IL electrolytes with different concentrations of LiTFSI.

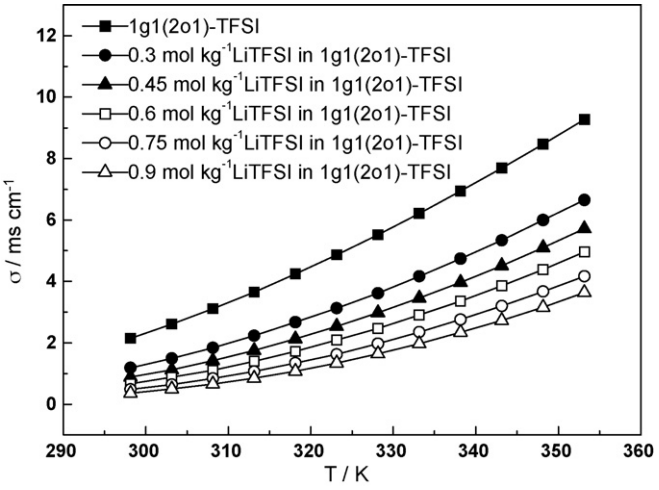

Fig. 3. Change of conductivity with temperature for 1g1(2o1)-TFSI without and with different concentrations of LiTFSI.

The temperature dependence of conductivity was also investigated for the IL and its IL electrolytes over the temperature range 25–80 °C, and the VTF plots of conductivity for them according to Eq. (2) were shown as examples in Fig. 3.

$$\sigma = \sigma_0 \exp\left(\frac{-B}{T - T_0}\right) \quad (2)$$

σ_0 (mS cm^{-1}), B (K) and T_0 (K) are constants of Eq. (2), and these three values and the VTF fitting parameter (R^2) for them were calculated and listed in Table 3. The temperature dependence of conductivity was also very well fit by the VTF model over the temperature range studied.

In terms of Table 3, the σ_0, B and T_0 values of the IL electrolytes with different concentrations of LiTFSI were bigger than the IL.

Table 2
VTF equation parameters of viscosity.

	η_0 (mPa s)	B (K)	T_0 (K)	R^2
1g1(2o1)-TFSI	0.149 (±6%)	768.3 (±2%)	169.3 (±1%)	0.999
0.3 mol kg^{-1} LiTFSI in 1g1(2o1)-TFSI	0.127 (±5%)	828.9 (±2%)	175.6 (±1%)	0.999
0.45 mol kg^{-1} LiTFSI in 1g1(2o1)-TFSI	0.130 (±5%)	819.9 (±1%)	181.5 (±1%)	0.999
0.6 mol kg^{-1} LiTFSI in 1g1(2o1)-TFSI	0.118 (±13%)	867.8 (±4%)	181.1 (±1%)	0.999
0.75 mol kg^{-1} LiTFSI in 1g1(2o1)-TFSI	0.136 (±4%)	808.9 (±1%)	188.8 (±1%)	0.999
0.9 mol kg^{-1} LiTFSI in 1g1(2o1)-TFSI	0.125 (±10%)	837.8 (±3%)	191.2 (±1%)	0.999

The percentage standard errors for η_0, B and T_0 have been included, and R^2 is the VTF fitting parameter.

Table 3
VTF equation parameters of conductivity.

	σ_0 (mS cm^{-1})	B (K)	T_0 (K)	R^2
1g1(2o1)-TFSI	155.9 (±2%)	455.4 (±1%)	191.8 (±1%)	0.999
0.3 mol kg^{-1} LiTFSI in 1g1(2o1)-TFSI	167.5 (±5%)	509.9 (±3%)	195.1 (±1%)	0.999
0.45 mol kg^{-1} LiTFSI in 1g1(2o1)-TFSI	164.5 (±4%)	517.0 (±3%)	199.3 (±1%)	0.999
0.6 mol kg^{-1} LiTFSI in 1g1(2o1)-TFSI	167.6 (±6%)	533.8 (±3%)	201.6 (±1%)	0.999
0.75 mol kg^{-1} LiTFSI in 1g1(2o1)-TFSI	179.9 (±6%)	567.1 (±3%)	202.4 (±1%)	0.999
0.9 mol kg^{-1} LiTFSI in 1g1(2o1)-TFSI	198.3 (±3%)	601.5 (±2%)	202.7 (±1%)	0.999

The percentage standard errors for σ_0, B and T_0 have been included, and R^2 is the VTF fitting parameter.

Obviously, the σ_0, B and T_0 values of the IL electrolytes showed explicit relationship with the concentrations of LiTFSI. The B and T_0 value of the IL electrolyte increased with the increasing of LiTFSI concentration, and the σ_0 value also increased with the increasing of LiTFSI concentration except the IL electrolyte with 0.3 mol kg^{-1} LiTFSI.

3.2. Lithium redox in the IL electrolytes

Fig. 4 shows the electrochemical window of this functionalized guanidinium IL at 25 °C, which is measured by LSV using lithium metal as reference electrode. The cathodic limiting potential of 1g1(2o1)-TFSI was about 0.7 V vs. Li/Li$^+$, and the anodic limiting potential was about 4.8 V vs. Li/Li$^+$. So its electrochemical window was about 4.1 V, which was almost identical with the value of this IL measured by using Ag as reference electrode [26]. The cathodic limiting potential vs. Li/Li$^+$ of 1g1(2o1)-TFSI was same as the two guanidinium IL without functional groups (1g13-TFSI and 1g22-TFSI), and close to imidazolium ILs [14,25,30].

According to the cathodic limiting potential of 1g1(2o1)-TFSI, it was very possible that their IL electrolytes could not allow the deposition of lithium without additives like the EMI-TFSI electrolyte [14]. But the CVs of the 1g1(2o1)-TFSI electrolytes with five different concentrations of LiTFSI at 25 °C are shown in Fig. 5(a)–(e), and the plating of lithium on Ni electrode can be clearly observed like the 1g13-TFSI and 1g22-TFSI electrolytes [25]. In the first cycle for the 1g1(2o1)-TFSI electrolyte with 0.3 mol kg^{-1} LiTFSI, the plating of lithium was at about −0.20 V vs. Li/Li$^+$, and the anodic peak at about 0.41 V in the returning scan corresponded to the stripping of lithium. The lithium redox in this electrolyte might be caused by the generation of a certain surface film (SEI) on the Ni electrode. The peak currents of the lithium redox decreased gradually with the cycle number, and it suggested that the SEI film changed so that the lithium redox was restrained markedly. The cathodic peak at about 0.30 V could be found in the first cycle. This cathodic peak might be assigned to the electrochemical reduction of the electrolyte, and at the same time it could be presumed that this reduction might generate the SEI film on Ni electrode. Furthermore, in the second and third cycles the current of this peak decreased, so it could mean that SEI film generating in the first cycle also restrained the reduction of the electrolyte.

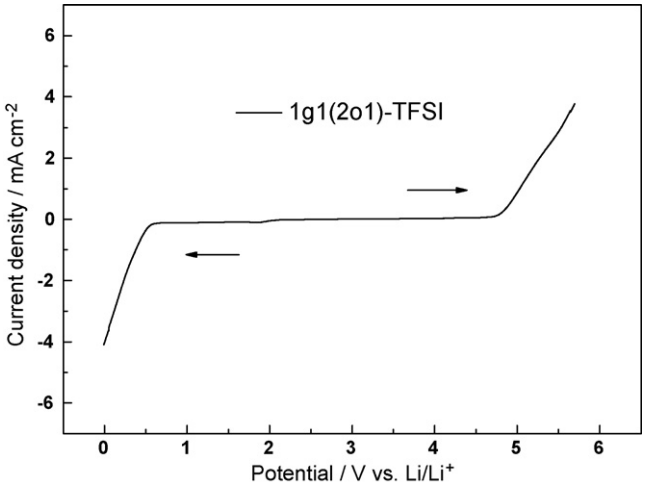

Fig. 4. Linear sweep voltammograms of 1g1(2o1)-TFSI at 25 °C. Working electrode: glassy carbon; counter electrode: Li; reference electrode: Li; scan rate: 10 mV s^{-1}.

It could be found in Fig. 5(a)–(e) that the LiTFSI concentration in the 1g1(2o1)-TFSI electrolytes distinctly affected the behaviors of lithium redox on the Ni electrode. Firstly, the peak currents of the lithium redox in the three cycles were different. If the ionic conductivities of these electrolytes were only taken into account, the electrolyte with 0.3 mol kg^{-1} LiTFSI should own bigger peak currents of the lithium redox due to its higher ionic conductivity. However, the peak currents for the electrolyte with 0.3 mol kg^{-1} LiTFSI were the smallest, which were obviously less than 1 mA cm^{-2}. The peak currents for the electrolytes with 0.45 and 0.6 mol kg^{-1} LiTFSI were bigger, which were more than 1 mA cm^{-2}. Secondly, the cathodic peaks of lithium for the electrolytes with 0.45, 0.6, 0.75 and 0.9 mol kg^{-1} LiTFSI almost overlapped in the three cycles, but the cathodic peaks of lithium for the electrolyte with 0.3 mol kg^{-1} of LiTFSI decreased gradually with the cycle number. Finally, how the anodic peaks of lithium changed with the cycle number was different for the electrolytes. For example, the anodic peaks of lithium for the electrolyte with 0.3 mol kg^{-1} LiTFSI decreased gradually with the cycle number, but the anodic peaks of lithium in the second cycle were higher than the anodic peaks of lithium in the first cycle for the electrolytes with 0.75 and 0.9 mol kg^{-1} LiTFSI.

3.3. Chemical stabilities of the IL electrolytes against lithium metal

Like N-n-butyl-N-ethylpyrrolidinium bis(trifluoromethanesulfonyl)imide (BEPy-TFSI), N-methoxyethyl-N-methylpyrrolidinium bis(trifluoromethanesulfonyl)imide ($PY_{1,2O1}$-TFSI), DEME-TFSI and DMPIm-TFSI electrolytes [18,23,31,32], the chemical stabilities of the 1g1(2o1)-TFSI electrolytes against lithium metal and the interfacial characteristics of IL electrolytes/lithium metal were investigated by electrochemical impedance spectra for symmetric Li/IL electrolyte/Li cells. Fig. 6(a) and (b) shows the time evolution of the impedance response of a symmetrical Li/0.3 mol kg^{-1} LiTFSI in 1g1(2o1)-TFSI/Li cell. The intercept with real axis of the response at high frequency was assigned to electrolyte bulk resistance, and the diameter of the semicircle was associated to the interfacial resistance (R_i) of the IL electrolyte/lithium metal. For the 1g1(2o1)-TFSI electrolyte with 0.3 mol kg^{-1} LiTFSI, its bulk resistance was almost unchangeable with time during 5 days. The R_i firstly increased and then fluctuated from 0 to 10 h, and the R_i retained about 200 Ω after 1 day. The cathodic limiting potential of 1g1(2o1)-TFSI was about 0.7 V Li/Li$^+$, so it was very possible that this IL electrolyte could continuously react with lithium metal. However, the experimental phenomena might indicate that the

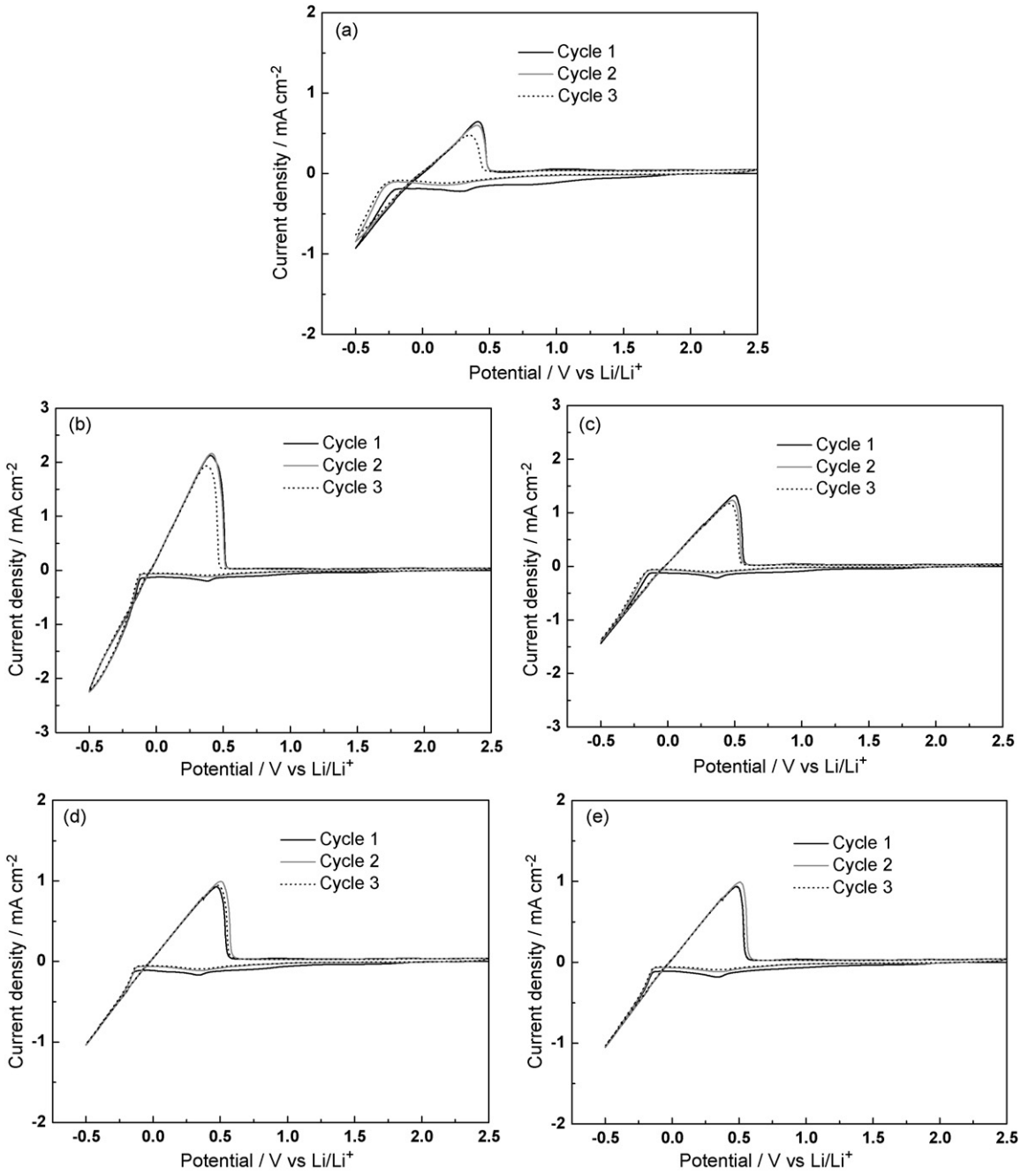

Fig. 5. Cyclic voltammograms for 1g1(2o1)-TFSI electrolytes with different concentrations of LiTFSI at 25 °C (−0.5 to 2.5 V vs. Li/Li^+): (a) 0.3 mol kg^{-1} LiTFSI; (b) 0.45 mol kg^{-1} LiTFSI; (c) 0.6 mol kg^{-1} LiTFSI; (d) 0.75 mol kg^{-1} LiTFSI; (e) 0.9 mol kg^{-1} LiTFSI. Working electrode: Ni; counter electrode: Li; reference electrode: Li; scan rate: 10 mV s^{-1}.

electrolyte reacted with lithium metal and a passivation layer could format at the same time. The passivation layer restricted the reaction between the electrolyte and lithium metal gradually, and a dynamic equilibrium could be achieved after some time.

Fig. 7(a) and (b) shows the time dependence of the interfacial resistance (R_i) of the Li/1g1(2o1)-TFSI electrolyte/Li cells. The R_i for the electrolyte with 0.45 mol kg^{-1} LiTFSI fluctuated more acutely from 0 to 12 h. When the R_i for all the five electrolytes were almost stable after 2 days, the R_i for the electrolyte with 0.3 mol kg^{-1} LiTFSI was smaller, and the electrolyte with 0.9 mol kg^{-1} LiTFSI had the biggest R_i value (about 2000 Ω). These results meant that the concentration of LiTFSI in 1g1(2o1)-TFSI electrolyte had an obvious effect on chemical reaction and interfacial characteristic between the electrolyte and lithium metal.

3.4. Charge–discharge characteristics of $Li/LiCoO_2$ cells

The C–D characteristics of $Li/LiCoO_2$ cells using the 1g1(2o1)-TFSI electrolytes without additives were examined at 0.2 C rate. Fig. 8 shows the discharge capacity during cycling of $Li/LiCoO_2$ cells. The initial discharge capacity of the cell using the electrolyte with 0.3 mol kg^{-1} LiTFSI was 130 mAh g^{-1}, and the discharge capacity at the 50th cycle was 103 mAh g^{-1}, which retained 79% of its initial capacity. The performance of the cell using this electrolyte was worse than the cells using 1g13-TFSI and 1g22-TFSI electrolytes with 0.3 mol kg^{-1} LiTFSI under the same experimental conditions

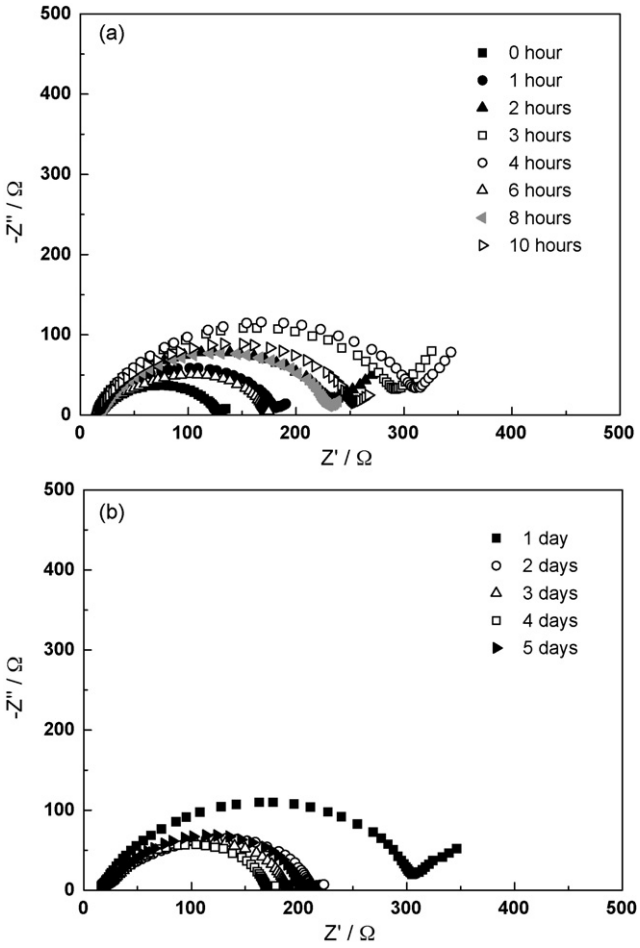

Fig. 6. Time evolution of the impedance response of a symmetrical Li/0.3 mol kg^{-1} LiTFSI in 1g1(2o1)-TFSI/Li cell: (a) from 0 to 10 h and (b) from 1 to 5 days.

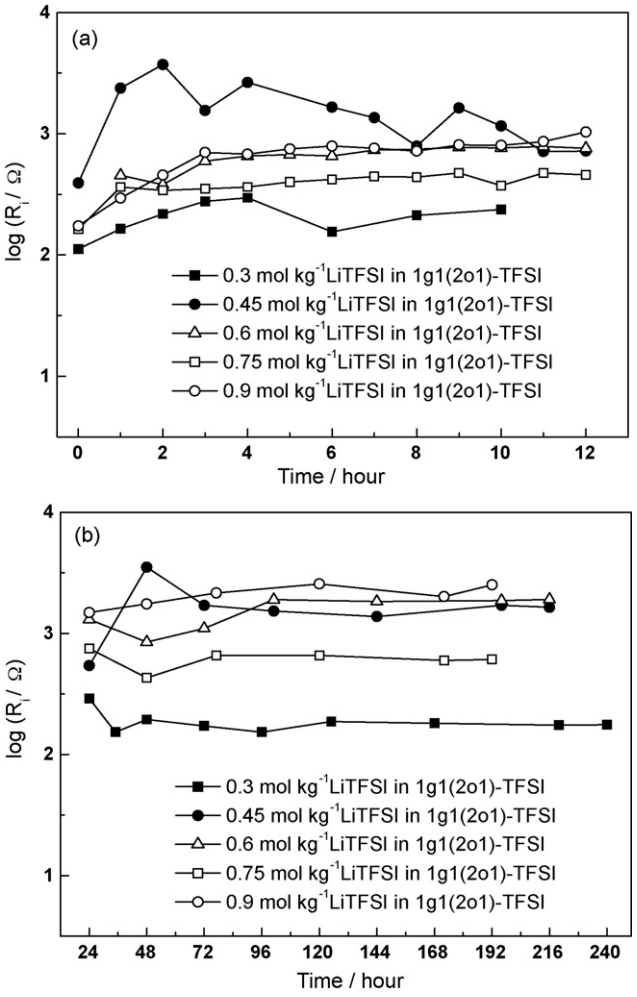

Fig. 7. Time dependence of interfacial resistance of the Li/1g1(2o1)-TFSI electrolytes/Li cells: (a) from 0 to 12 h and (b) from 24 to 240 h.

[25]. When the LiTFSI concentration in the 1g1(2o1)-TFSI electrolyte was higher than 0.3 mol kg^{-1}, the discharge capacity and cycle property of the cell improved obviously. For instance, the initial discharge capacity of the cell using the electrolyte with 0.9 mol kg^{-1} of LiTFSI was 143 mAh g^{-1}, and the discharge capacity at the 50th cycle was 129 mAh g^{-1}, which retained 90% of its initial capacity. Fig. 9 shows the cycle number dependence of coulombic efficiencies of Li/$LiCoO_2$ cells using these electrolytes at 0.2 C rate. Though the coulombic efficiencies of the five electrolytes were higher than 96% after the initial several cycles, the coulombic efficiency of the electrolyte with 0.3 mol kg^{-1} of LiTFSI was a little lower than the other electrolytes with the higher concentration of LiTFSI after the 15th C–D cycle. It indicated that, the electrolyte with 0.3 mol kg^{-1} LiTFSI might degrade more seriously during the C–D processes, and the higher concentration of LiTFSI could help to restrain the degradation of the electrolyte.

The relationships between the concentrations of LiTFSI in 1g1(2o1)-TFSI electrolytes and the discharge capacities at different current rates for Li/$LiCoO_2$ cells were examined, too. As shown in Fig. 10, it could be found that the discharge capacity decreased with the increasing of the current rate for the electrolytes containing different concentrations of LiTFSI. At the current rates of 0.2, 0.5 and 1.0 C, the discharge capacity increased with the increasing of the LiTFSI concentration. At the current rate of 1.5 C, the discharge capacity for the electrolyte with 0.75 mol kg^{-1} LiTFSI was highest. The rate property for the electrolyte with 0.3 mol kg^{-1} LiTFSI was unideal, and its discharge capacity at the current rate of 1.5 C was about 30 mAh g^{-1}, which was only 23% of the capacity at the current rate of 0.2 C. As shown in Fig. 11, the discharge capacity for the electrolyte with 0.75 mol kg^{-1} of LiTFSI at the current rate of 1.5 C was about 110 mAh g^{-1}, which retained 80% of the capacity at the current rate of 0.2 C, and this electrolyte owned the best rate property in the five electrolytes. Similar relationships between the concentrations of LiTFSI in DMPIm-TFSI electrolytes

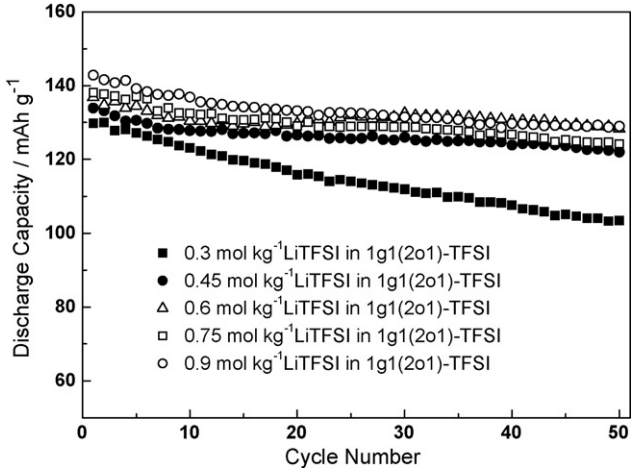

Fig. 8. Discharge capacity during cycling of Li/$LiCoO_2$ cells using the IL electrolytes with different concentrations of LiTFSI. Charge–discharge current rate is 0.2 C.

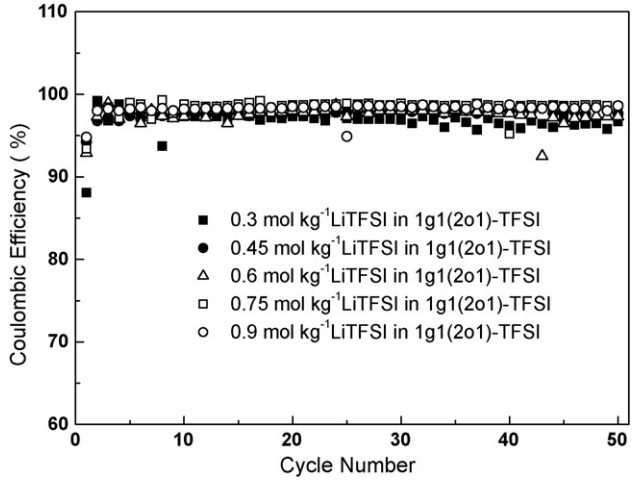

Fig. 9. The cycle number dependences of coulombic efficiency of $Li/LiCoO_2$ cell using the IL electrolytes with different concentrations of LiTFSI. Charge–discharge current rate is 0.2 C.

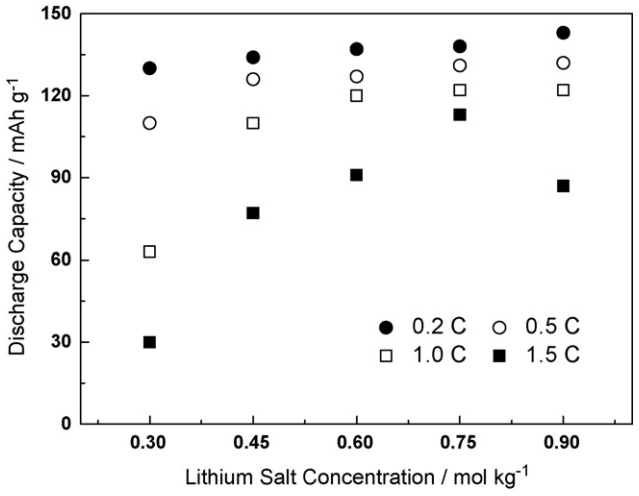

Fig. 10. Relationships between the concentrations of LiTFSI in 1g1(2o1)-TFSI electrolytes and the discharge capacities at different rates (0.2, 0.5, 1.0 and 1.5 C) for $Li/LiCoO_2$ cells.

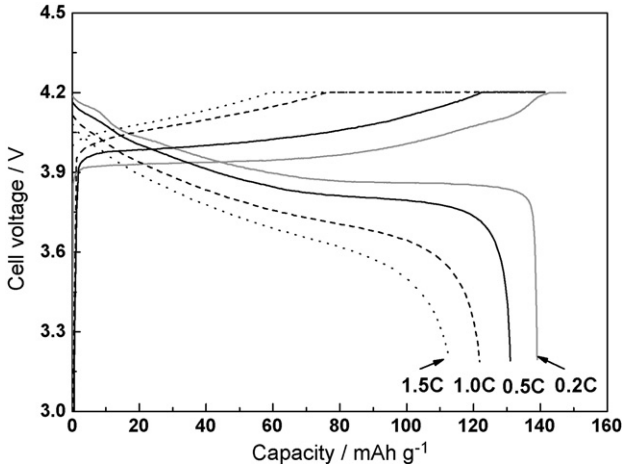

Fig. 11. Charge–discharge curves of $Li/LiCoO_2$ cells using 0.75 mol kg^{-1} LiTFSI in 1g1(2o1)-TFSI electrolyte. Charge–discharge current rate is indicated in this figure.

and the discharge capacities at different current rates for $Li/LiCoO_2$ cells have been observed, and some reasons have been tried to explain the phenomena: high concentration of lithium salt can supply more lithium ions at both the $LiCoO_2$ cathode/electrolyte and lithium metal anode/electrolyte interfaces, which is helpful to the rate property of cells; but high concentration of lithium salt can also reduce the transport capability of lithium ion in IL electrolyte, which is harmful to the rate property of cells; so an appropriate concentration of lithium salt in IL electrolyte can acquire better rate property of cells [23]. However, the interpretation based on the concentration and transport capability of lithium ion in IL electrolytes is not sufficient for the changing of rate property with the concentration of lithium salt, and it ignores the other factors, such as the interfacial characteristics at both the $LiCoO_2$ cathode/electrolyte and lithium metal anode/electrolyte interfaces.

3.5. Electrochemical kinetics

To investigate the cathode kinetics, the activation energies of the $LiCoO_2$ electrode for lithium intercalation were estimated by electrochemical impedance spectra using a previously reported method [10,33]. Fig. 12 shows the impedance response for $LiCoO_2$ electrodes in the cells using different electrolytes at a discharged potential of 3.85 V vs. Li/Li^+ at different temperatures after four C–D cycles. The semicircles in high-frequency and medium-frequency

Table 4
Charge transfer resistance (R_{ct}), exchange current (i_0) and apparent activation energies (E_a) for $LiCoO_2$ electrodes in the cells using different electrolytes at different temperatures.

Electrolytes	T (°C)	R_{ct} (Ω)	i_0 (A)	E_a (kJ mol^{-1})
0.3 mol kg^{-1} LiTFSI in 1g1(2o1)-TFSI	20	169.7	1.49×10^{-4}	70.48
	25	104.8	2.45×10^{-4}	
	30	67.9	3.85×10^{-4}	
0.45 mol kg^{-1} LiTFSI in 1g1(2o1)-TFSI	20	135	1.87×10^{-4}	72.28
	25	82.4	3.12×10^{-4}	
	30	52.8	4.95×10^{-4}	
0.6 mol kg^{-1} LiTFSI in 1g1(2o1)-TFSI	20	268.3	9.41×10^{-5}	60.27
	25	184.5	1.39×10^{-4}	
	30	123	2.12×10^{-4}	
0.75 mol kg^{-1} LiTFSI in 1g1(2o1)-TFSI	20	288.3	8.76×10^{-5}	63.13
	25	186.2	1.38×10^{-4}	
	30	127.4	2.05×10^{-4}	
0.9 mol kg^{-1} LiTFSI in 1g1(2o1)-TFSI	20	93.7	2.70×10^{-4}	67.04
	25	59	4.35×10^{-4}	
	30	39.2	6.66×10^{-4}	

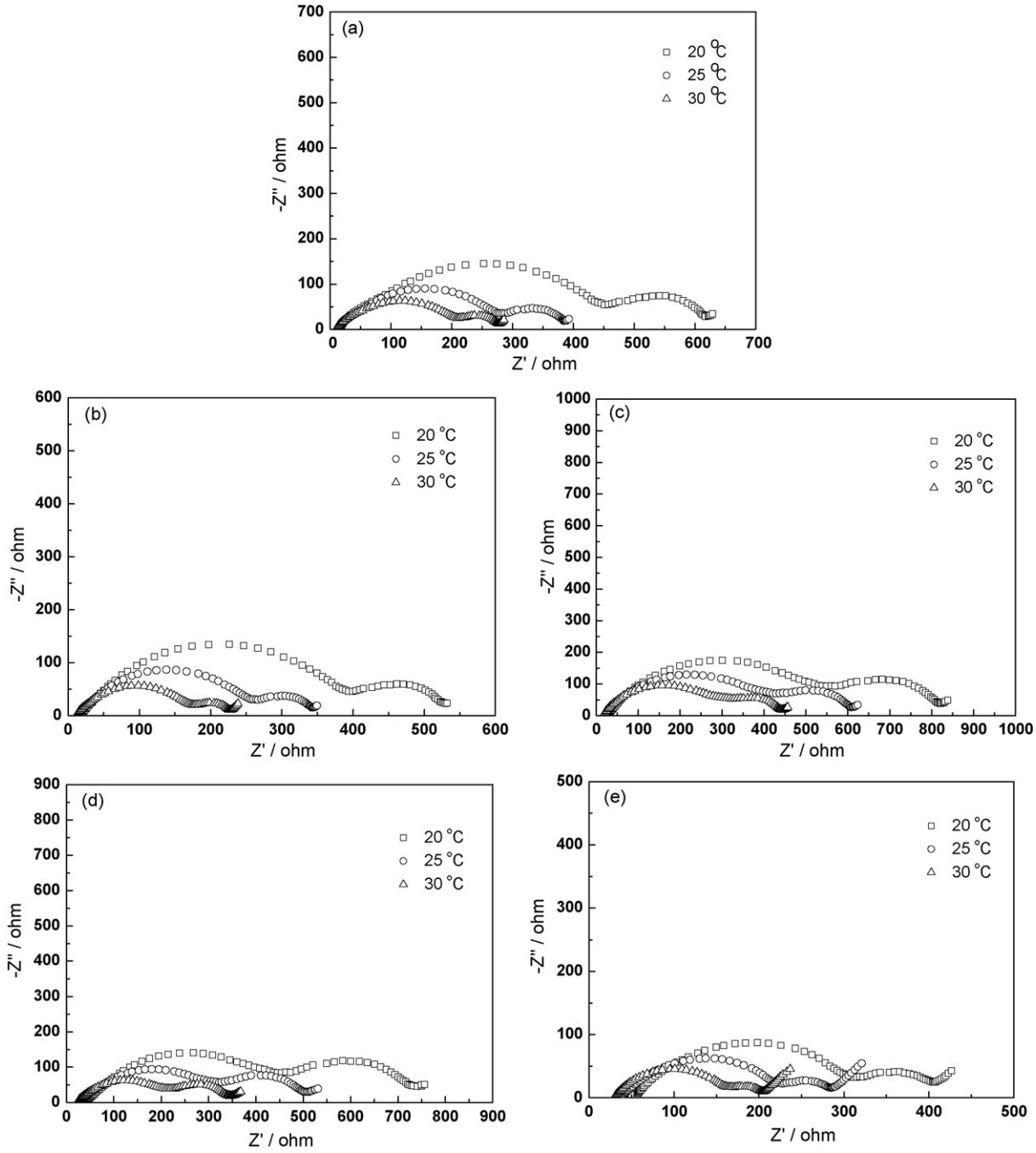

Fig. 12. Impedance response for $LiCoO_2$ electrodes in the cells using different IL electrolytes at a discharged potential of 3.85 V vs. Li/Li^+ at different temperatures: (a) 0.3 mol kg^{-1} LiTFSI in 1g1(2o1)-TFSI; (b) 0.45 mol kg^{-1} LiTFSI in 1g1(2o1)-TFSI; (c) 0.6 mol kg^{-1} LiTFSI in 1g1(2o1)-TFSI; (d) 0.75 mol kg^{-1} LiTFSI in 1g1(2o1)-TFSI; (e) 0.9 mol kg^{-1} LiTFSI in 1g1(2o1)-TFSI.

regions could be assigned to the $LiCoO_2$ electrode/electrolyte interface film resistance and the charge transfer resistance (R_{ct}). And the diameter of the semicircle in medium-frequency region was associated to the value of R_{ct}. The exchange current (i_0) and the apparent activation energies (E_a) for the lithium intercalation into $LiCoO_2$ could be calculated from Eq. (3) and the Arrhenius equation (Eq. (4)), respectively.

$$i_0 = \frac{RT}{nFR_{ct}} \tag{3}$$

$$i_0 = A \exp\left(\frac{-E_a}{RT}\right) \tag{4}$$

where A is a temperature-independent coefficient, R is the gas constant, T (K) is the absolute temperature, n is the number of transferred electrons, and F is the Faraday constant. The values of R_{ct} and i_0 for $LiCoO_2$ electrodes in the cells using different electrolytes at different temperatures were summarized in Table 4. Fig. 13 shows the Arrhenius plots of $\ln i_0$ as a function of $1/T$. The activation energies ($E_a = -Rk$, k = the slope of the fitting line in Fig. 13) for $LiCoO_2$ electrodes in the cells using different electrolytes were calculated, which also were listed in Table 4. The activation energy for the lithium intercalation at the interface of $LiCoO_2$ electrode/electrolyte might be determined by interfacial film, polarization of electrode and solvation of lithium ion in electrolyte. And the low activation energy for the lithium interca-

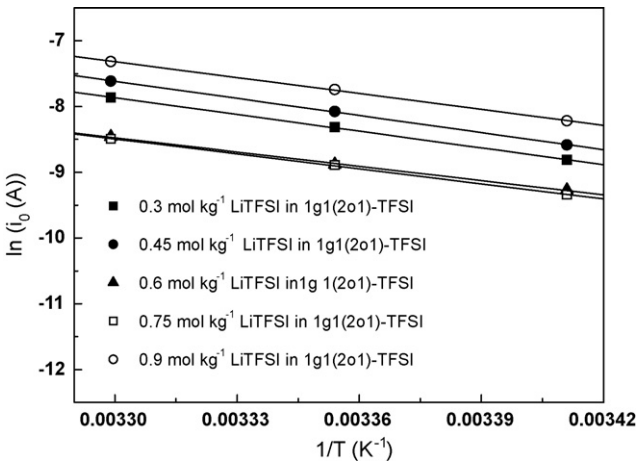

Fig. 13. Arrhenius plots of $\ln i_0$ vs. $1/T$ for the $LiCoO_2$ electrodes in the cells using different IL electrolytes at a discharged potential of 3.85 V vs. Li/Li^+.

lation into electrode meant quick electrochemical reaction velocity and high rate property. Though the 1g1(2o1)-TFSI electrolyte with 0.6 mol kg^{-1} LiTFSI owned lower activation energy, which was not consistent with the previous experimental result that the electrolyte with 0.75 mol kg^{-1} LiTFSI possessed better rate property, it indicated that the concentration and transport capability of lithium ion should affect the rate property besides interfacial film, polarization of electrode and solvation of lithium ion.

4. Conclusions

One ether-functionalized guanidinium IL (1g1(2o1)-TFSI) was used as new electrolyte for lithium battery. With the increasing of the LiTFSI concentration, the viscosity of IL electrolyte increased and the conductivity decreased. And the temperature dependences of conductivity and viscosity were very well fit by the VTF model for these IL electrolytes. Though the cathodic limiting potentials of the IL was higher than 0 V vs. Li/Li^+, the lithium plating and striping on Ni electrode could be observed in the IL electrolytes without additives due to the forming of SEI film. The IL electrolytes showed good chemical stability against lithium metal owing to the forming of passivation layer. $Li/LiCoO_2$ cells using the IL electrolytes without additive showed good discharge capacity and stable cycle property at 0.2 C current rate when the LiTFSI concentration in the IL electrolyte was higher than 0.3 mol kg^{-1}, and the cell using the IL electrolyte with 0.75 mol kg^{-1} LiTFSI owned good rate property. The activation energy for the lithium intercalation at the interface of $LiCoO_2$ electrode and IL electrolyte was affected by the LiTFSI concentration in electrolyte, which could help to analyze the factors determining the rate property of cells.

Acknowledgements

The authors thank the research center of analysis and measurement of Shanghai JiaoTong University for the help in the NMR characterization. This work was financially supported by the National Key Project of China for Basic Research under Grant No. 2006CB202600, the National High Technology Research and Development Program of China under Grant No. 2007AA03Z222, and Hitachi Chemical Co. Ltd.

References

[1] J. Sun, L.R. Jordan, D.R. MacFarlane, Electrochim. Acta 46 (2001) 1703.
[2] J. Dupont, R.F.D. Souza, P.A.Z. Suarez, Chem. Rev. 102 (2002) 3667.
[3] H. Sakaebe, H. Matsumoto, Electrochem. Commun. 5 (2003) 594.
[4] H. Matsumoto, H. Sakaebe, K. Tatsumi, M. Kikuta, E. Ishiko, M. Kono, J. Power Sources 160 (2006) 1308.
[5] M. Egashira, M.T. Nakagawa, I. Watanabe, S. Okada, J. Yamaki, J. Power Sources 160 (2006) 1387.
[6] M. Egashira, H. Todo, N. Yoshimoto, M. Morita, J. Yamaki, J. Power Sources 174 (2007) 560.
[7] L.X. Yuan, J.K. Feng, X.P. Ai, Y.L. Cao, S.L. Chen, H.X. Yang, Electrochem. Commun. 8 (2006) 610.
[8] J. Wang, S.Y. Chew, Z.W. Zhao, S. Ashraf, D. Wexler, J. Chen, S.H. Ng, S.L. Chou, H.K. Liu, Carbon 46 (2008) 229.
[9] J.Z. Wang, S.L. Chou, S.Y. Chew, J.Z. Sun, M. Forsyth, D.R. MacFarlane, H.K. Liu, Solid State Ionics 179 (2008) 2379.
[10] S. Chou, J. Wang, J. Sun, D. Wexler, M. Forsyth, H. Liu, D.R. MacFarlane, S. Dou, Chem. Mater. 20 (2008) 7044.
[11] S.Y. Chew, J.Z. Sun, J.Z. Wang, H.K. Liu, M. Forsyth, D.R. MacFarlane, Electrochim. Acta 53 (2008) 6460.
[12] H. Matsumoto, Y. Miyazaki, Chem. Lett. (2000) 922.
[13] K. Tsunashima, M. Sugiya, Electrochem. Commun. 9 (2007) 2353.
[14] H. Matsumoto, H. Sakaebe, K. Tatsumi, J. Power Sources 146 (2005) 45.
[15] H. Sakaebe, H. Matsumoto, K. Tatsumi, J. Power Sources 146 (2005) 693.
[16] H. Sakaebe, H. Matsumoto, K. Tatsumi, Electrochim. Acta 53 (2007) 1048.
[17] S. Seki, Y. Kobayashi, H. Miyashiro, Y. Ohno, Y. Mita, A. Usami, N. Terada, M. Watanabe, Electrochem. Solid-State Lett. 8 (2005) A577.
[18] S. Seki, Y. Ohno, H. Miyashiro, Y. Kobayashi, A. Usami, Y. Mita, N. Terada, K. Hayamizu, S. Tsuzuki, M. Watanabe, J. Electrochem. Soc. 155 (2008) A421.
[19] K. Tsunashima, F. Yonekawa, M. Sugiya, Chem. Lett. 37 (2008) 314.
[20] K. Tsunashima, F. Yonekawa, M. Sugiya, Electrochem. Solid-State Lett. 12 (2009) A54.
[21] K. Hayashi, Y. Nemoto, K. Akuto, Y. Sakurai, J. Power Sources 146 (2005) 689.
[22] F.F.C. Bazito, Y. Kawano, R.M. Torresi, Electrochim. Acta 52 (2007) 6427.
[23] S. Seki, Y. Ohno, Y. Kobayashi, H. Miyashiro, A. Usami, Y. Mita, H. Tokuda, M. Watanabe, K. Hayamizu, S. Tsuzuki, M. Hattori, N. Terada, J. Electrochem. Soc. 154 (2007) A173.
[24] S. Fang, L. Yang, C. Wei, C. Jiang, K. Tachibana, K. Kamijima, Electrochim. Acta 54 (2009) 1752.
[25] S. Fang, L. Yang, J. Wang, H. Zhang, K. Tachibana, K. Kamijima, J. Power Sources 191 (2009) 619.
[26] S. Fang, L. Yang, J. Wang, M. Li, K. Tachibana, K. Kamijima, Electrochim. Acta 54 (2009) 4269.
[27] Y. Saito, T. Umecky, J. Niwa, T. Sakai, S. Maeda, J. Phys. Chem. B 111 (2007) 11794.
[28] T. Frömling, M. Kunze, M. Schönhoff, J. Sundermeyer, B. Roling, J. Phys. Chem. B 112 (2008) 12985.
[29] K. Hayamizu, S. Tsuzuki, S. Seki, Y. Ohno, H. Miyashiro, Y. Kobayashi, J. Phys. Chem. B 112 (2008) 1189.
[30] J. Xu, J. Yang, Y. Li, J. Wang, Z. Zhang, J. Power Sources 160 (2006) 1308.
[31] A. Fernicola, F. Croce, B. Sceosati, T. Watanabe, H. Ohno, J. Power Sources 174 (2007) 342.
[32] S. Ferrari, E. Quartarone, P. Mustarelli, A. Magistris, S. Protti, S. Lazzaroni, J. Power Sources 194 (2009) 45.
[33] H. Ma, S. Zhang, W. Ji, Z. Tao, J. Chen, J. Am. Chem. Soc. 130 (2008) 5361.